

# THE TIMING, SIZE AND IMPACT OF AVALANCHES ON THE MILFORD HIGHWAY, NEW ZEALAND

H. Conway\*, W. Carran and A. Carran

University of Washington, U.S.A., and Works Infrastructure, TeAnau, New Zealand

**ABSTRACT:** The timing of direct-action avalanches that threaten the Milford Highway can often be predicted to within a few hours by keeping track of the stress from the new snowfall and the strength of sub-surface layers; avalanching is expected when the stress from the overburden exceeds the strength of a buried weak layer. For operational purposes it is also of interest to determine whether a particular avalanche will affect the highway. A flow model is used to calculate avalanche speeds and impact pressures. Although the model parameters are not well known, observations and model results indicate that the speed of an avalanche usually increases with size. The size of an avalanche depends on the initial depth of failure and subsequent entrainment/deposition of snow as it travels down the path. Avalanches gain mass above the snowline and lose mass below it; the size by the time it reaches the road depends on conditions in the track as well as the depth of the initial fracture. Keeping track of the snowline as well as the cumulative precipitation during storms may prove useful for predicting the size, speed and impact pressure from avalanches at road level.

**KEYWORDS:** Snow, avalanches

## 1. INTRODUCTION

The Milford Highway (SH-94) links TeAnau to Milford Sound on the southwest coast of New Zealand (Fig. 1). The highway, which follows the valley floor, is in the runout zone of avalanches that start more than 1000m higher. It is often difficult for travelers to perceive the hazard, especially on days when the snowline is well above the highway. The potential hazard from avalanches along the highway is well known (Smith, 1947; LaChapelle, 1979; Fitzharris and Owens, 1980; Fitzharris and Owens, 1984).

Average annual precipitation in the region exceeds 7m (w.e.) and winter storm cycles often deposit 2-3m of snow in the avalanche start zones. Most potentially hazardous avalanches are "direct-action" avalanches that release during or soon after storms. Rain is common, even during midwinter. Obtaining direct information about snow stability is problematic because access to the start zones during storms is not possible. Avalanche forecasters make decisions based on road-level observations of avalanche activity, measurements telemetered from remote weather stations, and weather forecasts issued by the NZ Meteorological Service. Control work and direct measurements of snow stability are restricted because of the need for fair weather for helicopter operations; when necessary, the hazard is managed by road closures.



Figure 1: Aerial view of the Milford Highway. The highway traverses up the Hollyford valley, passes through the Homer tunnel into the Cleddau valley, which it follows to Milford Sound. The highway is threatened by avalanches from both sides of both valleys.

\* Corresponding author address: Howard Conway, Geophysics Box 351659, University of Washington, Seattle, WA 98195, USA; tel: 206-685-8085; email: conway@geophys.washington.edu

There is increasing demand to keep the highway open year-round for tourist and fishing industries; there is strong motivation to improve predictions of the avalanche hazard. We recently developed a model of snow slope stability (SNOSS) as an aid to forecasting direct-action avalanche activity in maritime climates (Conway and Wilbour, 1999). Here we apply the model to the Milford highway. For operational purposes it is not only of interest to determine when an avalanche will release, but also whether it will affect the highway. As a first step toward addressing this issue we investigate the suitability of a one-dimensional dynamic flow model for estimating avalanche speeds and impact pressures at road level.

## 2. MODEL DEVELOPMENT

### 2.1 *Snow slope stability*

A necessary condition for slab avalanche release is that the shear stress from the overburden exceeds the shear strength of a buried weak layer; slopes are potentially unstable when the stress exceeds the strength (Perla and LaChapelle, 1970; McClung, 1981). Hourly measurements of air temperature, precipitation and winds telemetered from remote weather stations are used to track the evolution of the force balance. The strength of a buried layer is calculated from its density; the density of new snow is estimated from measurements of air temperature and subsequent metamorphism and compaction is calculated by assuming viscous behavior. The shear stress is calculated from the cumulative precipitation and the slope angle. Output from SNOSS is the depth of the avalanche as well as the time of release (Conway and Wilbour, 1999).

### 2.2 *Snow in motion*

Assuming an avalanche can be characterized as a finite mass  $M$  of snow moving down slope, the change in momentum is governed by the body forces  $F$  (Perla et al. 1980):

$$\frac{d}{dt}(Mv) = \sum F \quad (1)$$

Body forces are gravity (driving the flow), and resisting forces that include terms for drag, ploughing and friction. It is mathematically convenient to sub-divide a path into discrete lengths of constant slope and resistance. Acceleration of the flow from its initial position at rest at the top of the start zone is calculated from eqn. 1. The speed leaving the first

segment is then used to determine the initial speed for the second segment and the calculation is repeated for the next segment until  $v_i = 0$ , which defines the run-out distance. The speed at road level  $v_H$ , combined with the density of the flow  $\rho_F$ , provide an estimate of the impact pressure at road level:

$$I_H \approx \rho_F v_H^2 \quad (3)$$

An advantage of this type of model is that it is easily applied to engineering problems. A disadvantage is that the model parameters (the resisting forces and the flow density) down a path are not well known. Here we investigate the utility of such a model for operational forecasting.

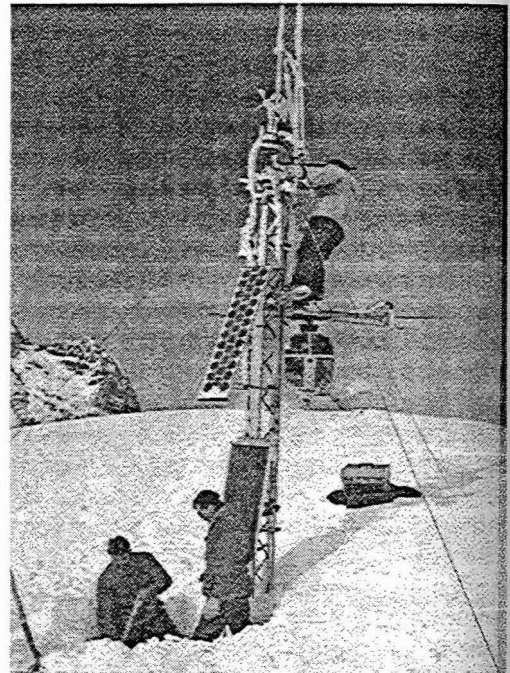


Figure 2: Weather station at Mt Belle (1600m), one of five remote weather stations in the region.

## 3. APPLICATION TO MILFORD HIGHWAY

### 3.1 *Weather and avalanche database*

Hourly measurements of winds, precipitation, and air temperature that are needed for input to SNOSS are telemetered from a network of five remote weather stations to a base station in TeAnau (Fig.2). Air temperature at a particular elevation  $T_z$  is estimated from  $T_{1600}$  measured at the Mt Belle weather station and the moist adiabatic lapse rate ( $5.5^\circ\text{Ckm}^{-1}$ ). We

assume that precipitation falls as snow when the air temperature is  $<2^{\circ}\text{C}$  and rain otherwise; the snowline (at the elevation where  $T_z = 2^{\circ}\text{C}$ ) is  $\sim 360\text{m}$  below the freezing level. We have found that the most reliable measurements of precipitation come from the East Homer precipitation gauge (900m) and these are used to estimate the shear stress in the start zones. Model output is compared with observations of the time of avalanche activity and measurements of snow stratigraphy recorded at fracture lines and snow pits.

### 3.2 *Terrain, speed and impact pressure*

More than 50 avalanche paths threaten the Milford highway (Fitzharris and Owens, 1980). Most paths are steep (35-45°) and long (more than 1km); Fig. 3 shows profiles of three paths. Speeds have been measured from video-footage taken during helicopter-bombing missions (Fig. 4); speeds across the highway often exceed  $60\text{ms}^{-1}$  (McLauchlan, 1995). Impact pressures have not been measured directly, but order of magnitude estimates of forces are available from observations of damage to trees and reinforced concrete structures (Fig. 5).

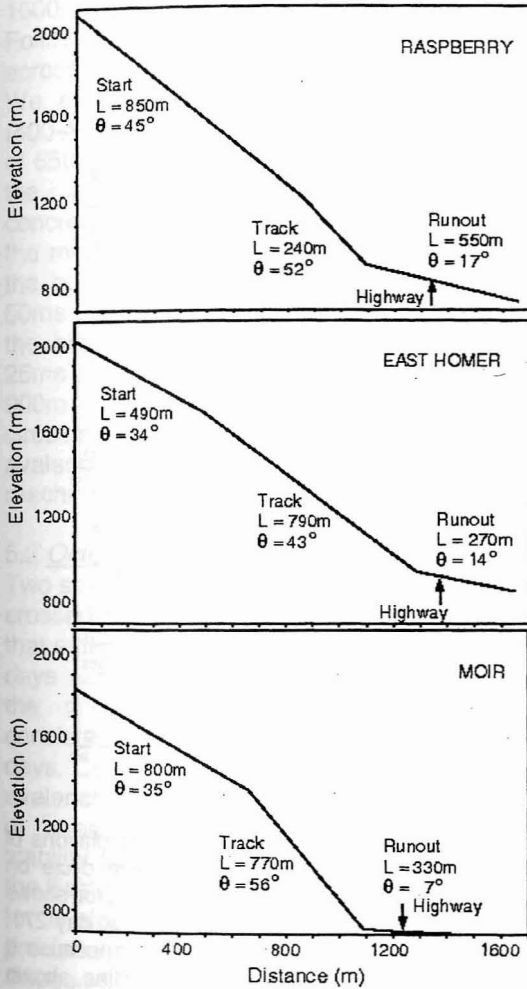


Figure 3: Profiles of the Raspberry, East Homer and Moir avalanche paths (adapted from Fitzharris and Owens, 1980). The Raspberry path is steeper than East Homer but the highway is farther from the end of the track (250m compared to 90m at East Homer). The elevation of the highway beneath Moir on the west side (700m) is about 200m lower than that on the east side.

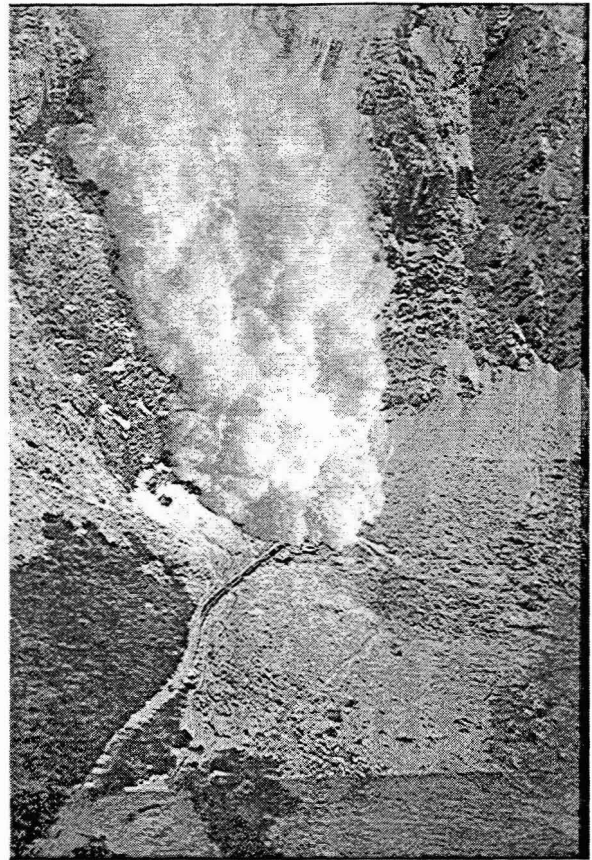


Figure 4: Artificially released avalanche down the East Homer path hitting the entrance to the Homer tunnel.

We make use of these observations to estimate values for the model parameters (friction, dynamic drag and flow density) that are needed to calculate avalanche speeds and impact pressures. A reasonable range of values for the bed friction is  $0.1 \leq \mu \leq 0.5$ ,

depending on factors such as snow type, path roughness and the presence of trees. Sensitivity studies indicate the model is more sensitive to values chosen for the dynamic drag, which probably varies from about  $10^2\text{m}$  for wet avalanches to more than  $10^4\text{m}$  for large dry avalanches (Perla et al. 1980). As a first approximation we assign  $\mu = 0.2$  in the start zones,  $\mu = 0.3$  in the tracks and  $\mu = 0.4$  in the runout zones. The choice of values for the dynamic drag is guided by the moisture content and the mass of the avalanche. Moisture content in each segment of the path is estimated from the snowline elevation during the storm. The snowline is also used to determine whether an avalanche will entrain or deposit snow in each segment of the path; as a first approximation we assume that an avalanche will entrain all of the new snow above the snowline, and loose 100mm/m below it. In reality not all of the new snow will be entrained, and the mass loss will depend on the roughness of the path at the time of avalanching. The density of the flow is expected to range from  $\sim 10\text{kgm}^{-3}$  for powder avalanches, to  $200\text{--}550\text{kgm}^{-3}$  for flowing avalanches (McClung and Schaerer, 1993).



Figure 5: An avalanche on October 7, 1996 damaged the east portal of Homer tunnel. Impact pressures of  $\sim 1000\text{kPa}$  are needed to damage reinforced-concrete structures (McClung and Schaerer, 1993).

#### 4. MODEL RESULTS

We illustrate the application of the two models by comparing results with observations during two contrasting storm and avalanche cycles. During one storm more than 600mm of precipitation was measured, while during the other there was only 80mm. In both cases avalanches reached the highway.

#### 4.1 October 7 (Day 281) 1996

Several large ( $>2.5$ ), natural avalanches released some time before 0600 on day 281, and a large avalanche at 0900 down the East Homer path damaged the portal of the Homer tunnel (Fig.4). All paths had slid either naturally or during control missions on days 262 and 263, which would have eliminated most of the deep instability in the snowpack.

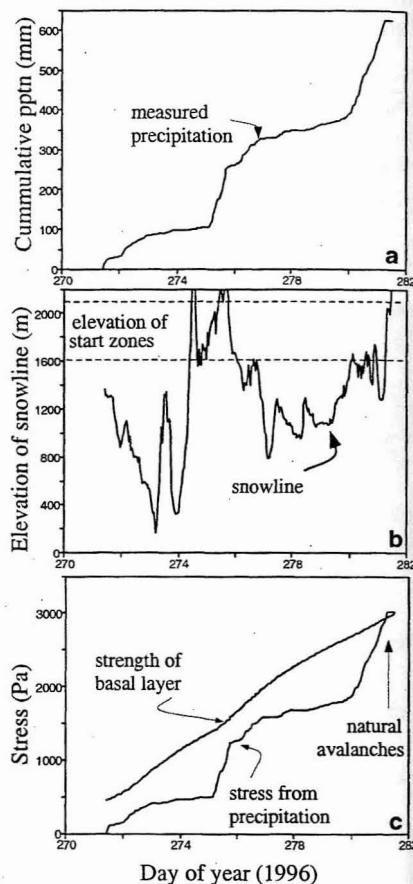


Figure 6: Measurements and model calculations of conditions leading up to the avalanche cycle on October 7, 1996 (day 281). The upper plot shows the cumulative precipitation since 1000 on day 271; no new snow accumulated before then because it was raining in the start zones. The snowline, shown in the middle plot indicates rain probably fell in the start zones ( $\sim 2000\text{m}$  elevation) late on day 271. Failure is predicted at 0500 on day 281, which coincides closely with the timing of the natural avalanches, and is several hours before the large avalanche on East Homer.

Fig. 6 shows conditions during the 10 days prior to the avalanches. The cumulative precipitation during the storm was 630mm (Fig. 6a), which compares well with

measurements that showed the fracture at East Homer was 1.35m deep with an average density of  $450\text{kgm}^{-3}$  (610mm water equivalent). SNOSS predicts failure at 0500 on day 281, which coincides closely with the timing of the natural avalanches; it is several hours before the large avalanche on East Homer.

Although a large amount of snow failed initially, the snowline was generally high for most of the storm and near 1600m for 24 hours prior to avalanching. We assume that the avalanche gained mass (630mm/m) above 1600m and lost mass (100mm/m) below. Following these assumptions, the speed across the highway at East Homer is  $40\text{ms}^{-1}$ . We expect the flow to be relatively dense ( $400\text{-}450\text{kgm}^{-3}$ ), resulting in impact pressures of 650-700kPa, which is reasonable given that the avalanche damaged the reinforced concrete portal of the Homer tunnel. Although the modeled speed on Raspberry is faster at the bottom of the track ( $55\text{ms}^{-1}$  compared to  $50\text{ms}^{-1}$  on East Homer), by the time it crossed the highway it would have slowed to about  $25\text{ms}^{-1}$ . In the case of Moir, the snowline was 900m above the highway; under these circumstances the model predicts that any avalanches that started would stop before reaching the highway.

### 5.2 October 5 (Day 278) 1998

Two size 3 avalanches (East Homer and Moir) crossed the highway on day 278. It is likely that extensive control work with explosives two days earlier eliminated any deep instability in the snowpack and that the avalanches consisted only of the snow of the previous two days. Conditions for the two days prior to the avalanches are shown in Fig. 7. The evolution of stress and strength indicates minimum stability (but not failure) about 7 hours before the East Homer avalanche. Results plotted are for a slope of  $40^\circ$  and no enhancement of precipitation; the model predicts failure of slopes  $>55^\circ$ , or at locations where precipitation in the start zones was only 10% higher than that measured at road level.

Cold temperatures and the low cumulative precipitation at the time of failure (80mm w.e.) suggest that the initial fractures would be relatively small and dry. However snow at low elevations (the snowline was  $\sim 900\text{m}$  during most of the storm) would be entrained and avalanches would increase in size as they traveled down the track. Model calculations

indicate speeds of  $\sim 45\text{ms}^{-1}$  at the bottom of the East Homer track slowing to  $35\text{ms}^{-1}$  across the highway. In this case we expect a relatively low flow density ( $10\text{-}50\text{kgm}^{-3}$ ) and impact pressures of 10-60kPa, which are still sufficient to damage a vehicle. Applying the same rules for an avalanche down the Moir slide path yields a speed of  $40\text{ms}^{-1}$  at the bottom of the track that decreases to  $10\text{ms}^{-1}$  across the highway. Size 3.0 avalanches on both these paths crossed the highway at the end of the storm (Fig. 7). Although none were observed, the model predicts that avalanches down the Raspberry path would also cross the highway ( $v_H = 20\text{ms}^{-1}$ ).

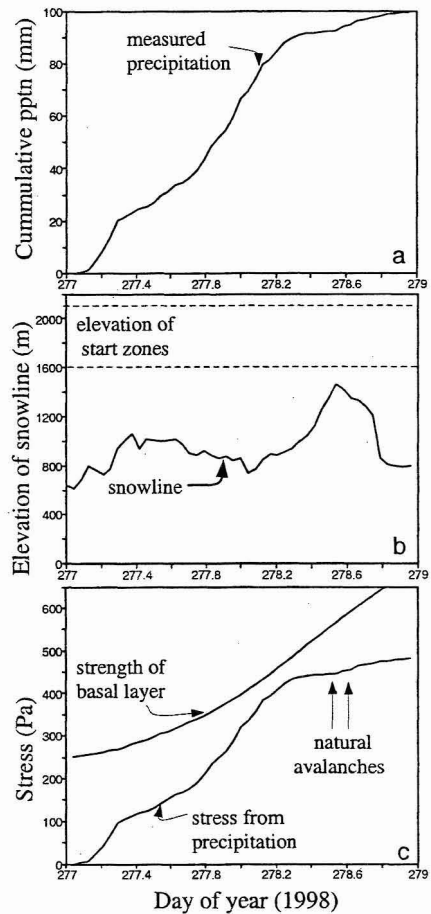


Figure 7: Precipitation started at 0200 on day 277. The snowline remained below 900m during most of the storm; snow would have accumulated in the tracks of most avalanche paths. The evolution of stress and strength indicates minimum stability (but not failure) about 7 hours before the East Homer avalanche.

## 5. CONCLUSIONS

We have now tested SNOSS using numerous avalanche cycles in maritime climates and we are encouraged that it appears to predict the time of direct-action avalanching to within a few hours. We had thought that influences such as longitudinal stress gradients in the slab, non-linear and time-dependent properties of snow, and/or spatial variations in basal strength would limit the success of such an approach; we are not certain that the model would be so successful in regions where slope stability is more strongly influenced by the slab strength, or in cases of deep, persistent instability.

Tests using a one-dimensional dynamic flow model are also encouraging. We caution, however, that values for the model parameters are not well known and nor are they unique. Further work is necessary to better define these parameters. Nevertheless, sensitivity studies indicate that the speed of an avalanche depends strongly on the dynamic drag, which depends on the size; other things being equal, larger, dry snow avalanches travel faster. The size at road level depends not only on the initial depth of fracture but also on subsequent entrainment or deposition of snow down the path. Avalanches will gain mass above the snowline but lose mass below it. Monitoring the snowline as well as the cumulative precipitation during storms may prove useful for predicting the mass and hence the speed and potential hazard at road level.

## 6. REFERENCES

- Conway, H. and C. Wilbour, 1999. Evolution of snow slope stability during storms. *Cold Reg. Sci. and Tech.*, 30(1-3), 67-77.
- Fitzharris, B.B. and I.F. Owens, 1980. Avalanche atlas of the Milford road and an assessment of the hazard to traffic. *NZ Mountain Safety Council Avalanche Committee Report No. 4.*
- Fitzharris, B.B. and I.F. Owens, 1984. Avalanche tarns. *J. Glaciol.*, 30(106), 308-312.
- LaChapelle, E.R. 1979. An assessment of avalanche problems in New Zealand. *NZ Mountain Safety Council Avalanche Committee Report No. 2.*
- McClung, D.M. 1981. Fracture mechanical models of dry slab avalanche release. *J. Geophys. Res.*, 86(B11), 10783-10790.

- McClung, D.M and P.A. Schaerer, 1993. The Avalanche Handbook. *The Mountaineers, Seattle, WA.*, 271 pp.
- McLauchlan, H.J., 1995. An assessment of the velocities, impact pressure and other related effects of the avalanches on the Milford road, Fiordland, New Zealand. *Unpublished Ms thesis, U. Canterbury, New Zealand.*
- Perla R. and E.R. LaChapelle, 1970. A theory of snow slab failure. *J. Geophys. Res.*, 75(36), 7619-7627.
- Perla, R., T.M. Beck and T.T. Cheng, 1982. The shear strength index of alpine snow. *Cold Reg. Sci. and Tech.*, 6(1), 11-20.
- Smith, H.W., 1947. Avalanches. *NZ Eng.*, 2(5), 491-496.

## 7. ACKNOWLEDGEMENTS

Works Infrastructure and Transit New Zealand funded and supported this work. We also thank all the people who have worked on the Milford highway. Their dedication and observations made this research possible.